

As a library, NLM provides access to scientific literature. Inclusion in an NLM database does not imply endorsement of, or agreement with, the contents by NLM or the National Institutes of Health.

Learn more: [PMC Disclaimer](#) | [PMC Copyright Notice](#)

Preprint

Made publicly accessible prior to peer review



Version 1. [bioRxiv](#). Preprint. 2022 Dec 26.

PMCID: PMC9810210

doi: [10.1101/2022.12.25.521784](#)

PMID: [36597527](#)

This is a preprint.

It has not yet been peer reviewed by a journal.

The National Library of Medicine is [running a pilot](#) to include preprints that result from research funded by NIH in PMC and PubMed.

A ferritin-based COVID-19 nanoparticle vaccine that elicits robust, durable, broad-spectrum neutralizing antisera in non-human primates

[Payton A.-B. Weidenbacher](#)^{1,2,‡} [Mrinmoy Sanyal](#)^{1,3,‡} [Natalia Friedland](#)^{1,3,‡} [Shaogeng Tang](#)^{1,3}
[Prabhu S. Arunachalam](#)⁴ [Mengyun Hu](#)⁴ [Ozan S. Kumru](#)⁵ [Mary Kate Morris](#)⁶ [Jane Fontenot](#)⁷ [Lisa Shirreff](#)⁷
[Jonathan Do](#)^{1,3} [Ya-Chen Cheng](#)^{1,3} [Gayathri Vasudevan](#)⁸ [Mark B. Feinberg](#)⁸ [Francois J. Villinger](#)⁷ [Carl Hanson](#)⁶
[Sangeeta B. Joshi](#)⁵ [David B. Volkin](#)⁵ [Bali Pulendran](#)^{4,9,10} and [Peter S. Kim](#)^{1,3,11,*}

Abstract

While the rapid development of COVID-19 vaccines has been a scientific triumph, the need remains for a globally available vaccine that provides longer-lasting immunity against present and future SARS-CoV-2 variants of concern (VOCs). Here, we describe DCFHP, a ferritin-based, protein-nanoparticle vaccine candidate that, when formulated with aluminum hydroxide as the sole adjuvant (DCFHP-alum), elicits potent and durable neutralizing antisera in non-human primates against known VOCs, including Omicron BQ.1, as well as against SARS-CoV-1. Following a booster one year after the initial immunization, DCFHP-alum elicits a robust anamnestic response. To enable global accessibility, we generated a cell line that can enable production of thousands of vaccine doses per liter of cell culture and show that DCFHP-alum maintains potency for at least 14 days at temperatures exceeding standard room temperature. DCFHP-alum has potential as a once-yearly booster vaccine, and as a primary vaccine for pediatric use including in infants.



INTRODUCTION:

The COVID-19 pandemic was met with record-breaking vaccine development speed,^{1,2} and widespread vaccination is estimated to have prevented over 14 million deaths in the first year of implementation.³ Nonetheless, there remains an urgent public health need for vaccine interventions. First, as of May, 2022, the WHO estimates that almost one billion people globally remain unvaccinated against SARS-CoV-2.⁴ Second, affordability continues to be an obstacle to global vaccine accessibility, including the cost of low-temperature storage and transport.^{5,6} Third, the protection against infection provided by vaccine-induced or infection-induced immunity wanes with time, which has led to frequent booster vaccine doses.⁷ Fourth, SARS-CoV-2 variants of concern (VOCs) capable of evading natural or vaccine-induced humoral immunity continue to emerge.⁸ Finally, as SARS-CoV-2 becomes endemic, worldwide immunization of the pediatric population, including of infants, remains an unmet need.⁹

Protein nanoparticle vaccines, compared to isolated protein subunits, are more readily taken up by antigen-presenting dendritic cells^{10,11} and the multivalent presentation of the antigen facilitated by the nanoparticles promotes receptor clustering and subsequent activation of B cells.^{12,13} Indeed, candidate ferritin-based nanoparticle vaccines have shown robust humoral immune responses against SARS-CoV-2¹⁴⁻¹⁶ and other viral glycoproteins,¹⁷⁻²¹ including showing safety and efficacy in clinical trials.^{20,22} Previously, we introduced a protein nanoparticle-based vaccine candidate, SΔC-Fer, which displays a truncated form of the prefusion SARS-CoV-2 spike-protein ectodomain trimer from the Wuhan-1 isolate on self-assembling *Helicobacter pylori* ferritin nanoparticles.¹⁴ SΔC-Fer contains a mutated furin cleavage site and the 2-proline (2P)²³ prefusion-stabilizing substitutions found in the FDA-approved SARS-CoV-2 mRNA vaccines.^{1,24} Importantly, SΔC-Fer also contains a deletion of 70 amino acid residues from the C-terminus of the spike ectodomain. This deletion removes a highly flexible region that is not well resolved in cryo-EM structures^{25,27}, and that contains immunodominant, linear (i.e., not conformational) epitopes frequently targeted by antibodies in convalescent COVID-19 plasma^{28,29}. Removal of these immunodominant linear epitopes and multivalent presentation of the modified spike protein on a ferritin nanoparticle substantially improved the neutralizing potency of elicited antisera relative to other tested vaccines in mice¹⁴.

Here, we introduce an updated version of SΔC-Fer, called Delta-C70-Ferritin-HexaPro or DCFHP. We supplemented the 2P stabilizing substitutions with four previously described²⁶ proline substitutions to create a six-proline substituted (HexaPro) version of the vaccine. Previous work has shown that the HexaPro SARS-CoV-2 spike protein has increased stability and expression relative to the 2P version²⁶. We found that DCFHP is more stable to thermal denaturation than SΔC-Fer. In addition, we show that DCFHP can be generated in a Chinese hamster ovary (CHO) cell line at levels exceeding 2 grams per liter.

Our vaccine formulation, DCFHP-alum, consists of DCFHP antigen formulated with aluminum hydroxide (Alhydrogel™, referred to herein as alum) as the only adjuvant.³⁰ Aluminum salt adjuvants are the most commonly used adjuvant in human vaccines licensed by the FDA and regulatory agencies worldwide, and have been administered to billions of individuals over the past 90 years^{31,33}.

Moreover, aluminum salt adjuvants are currently used in infant vaccines against hepatitis B, diphtheria-tetanus-pertussis (DTaP), *Haemophilus influenzae* type b (Hib), and pneumococcus infectious agents³⁴, with an excellent safety profile.^{35,36}

We show here that DCFHP-alum elicits a robust and durable immune response in mice against SARS-CoV-2 VOCs. Additionally, we demonstrate that DCFHP-alum remains stable at temperatures ranging from 4°C to 37°C for at least 14 days, as assessed by immunization studies in mice. Thus, we anticipate that local distribution of the DCFHP-alum vaccine could be feasible without refrigeration.

Finally, we demonstrate that a two-dose intramuscular immunization regimen in rhesus macaques with DCFHP-alum elicits antisera with durable, robust and broad neutralization of VOCs, including the Omicron subvariants BA.4/5³⁷ and BQ.1,³⁸ along with a balanced Th1 and Th2 immune response. Strikingly, these non-human primate (NHP) antisera also show robust and durable neutralization activity against the phylogenetically divergent SARS-CoV-1 pseudovirus.³⁹ Boosting these immunized NHPs after ~1 year with a third dose of DCFHP-alum elicits a robust, broad-spectrum, anamnestic neutralizing antibody response. Taken together, these results suggest that DCFHP-alum may provide an affordable and effective solution to pediatric and worldwide vaccination against SARS-CoV-2 and present the possibility of an effective, once-yearly booster.

RESULTS:

Vaccine design and characterization

We sought to further optimize our ferritin-based nanoparticle vaccine, SΔC-Fer,¹⁴ to generate DCFHP, which includes additional stabilizing proline residues to promote robust expression. DCFHP maintains the 2P substitutions²³ and deletion of 70 C-terminal spike ectodomain residues contained in SΔC-Fer,¹⁴ but also incorporates four proline residue substitutions and a modification to the mutated furin cleavage site, as described in the HexaPro spike design²⁶ (Fig 1A). As expected, DCFHP is expressed at higher levels than SΔC-Fer following transient transfection in Expi293F cells (SI Fig 1A–B). SDS-PAGE analysis of purified DCFHP showed the expected monomeric molecular weight of ~160kDa (Fig 1B). Additionally, size-exclusion chromatography coupled with multiangle light scattering (SEC-MALS) analysis shows that the nanoparticle has a molecular weight (~3.4MDa) consistent with a ferritin-based nanoparticle displaying eight copies of the SARS-CoV-2 spike ectodomain trimer (Fig 1C). Differential scanning fluorimetry (DSF) experiments indicate that thermal denaturation of DCFHP occurs at higher temperatures compared to SΔC-Fer, and these changes are similar to those observed between the 2P and HexaPro variants of the spike trimer²⁶ (SI Fig 1C), suggesting that HexaPro mutations induce similar stabilizing effects in the context of the nanoparticle. Biolayer interferometry (BLI) binding of conformation-specific antibodies^{40–43} indicates proper epitope presentation (SI Fig. 1D). Finally, single particle cryo-electron microscopy (cryo-EM) of DCFHP shows a multivalent particle displaying eight copies of the SARS-CoV-2 trimer arrayed radially from a ferritin core (Fig 1D, SI Fig. E–F), as was observed previously with SΔC-Fer.¹⁴ Collectively, these data suggest that the spike component of DCFHP maintains the same native conformation as in SΔC-Fer, with increased stability and expression levels conferred by the HexaPro substitutions.

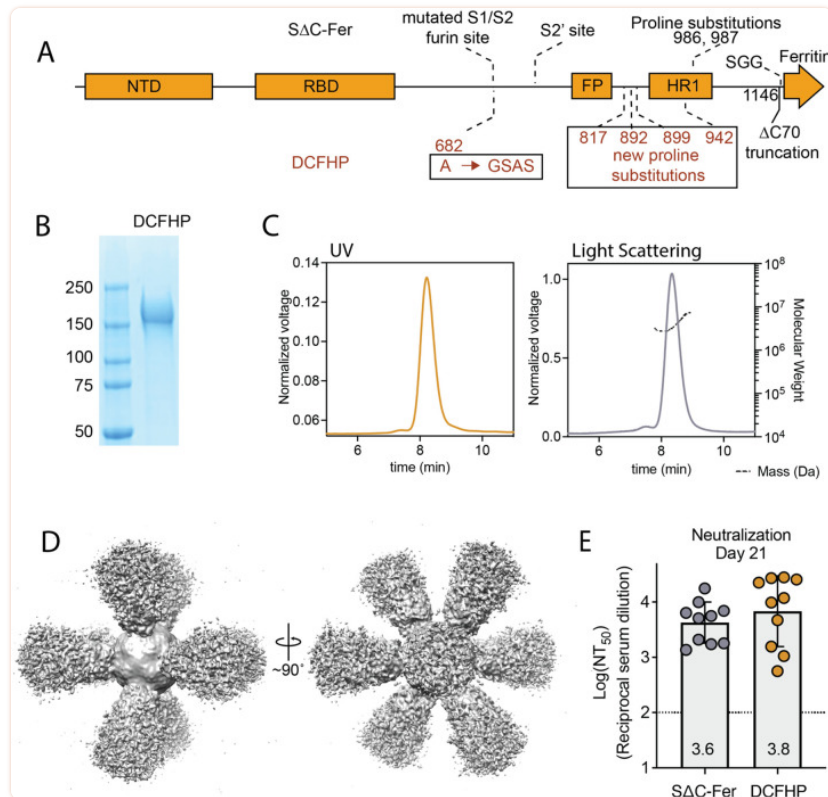


Figure 1 –

DCFHP design and validation. (A) DCFHP schematic showing the modifications made to convert SΔC-Fer into DCFHP in red. Receptor binding domain (RBD), N-terminal domain (NTD), S1/S2 cleavage site, S2' cleavage site, fusion peptide (FP), heptad repeat 1 (HR1), as annotated. (B) SDS-PAGE gel showing purified DCFHP running as a monomer at the anticipated kDa molecular weight (ladder, shown left). (C) UV (yellow) and light scattering (grey) traces determined from SEC-MALS shows a homogenous nanoparticle peak with approximate molecular weight (dashed line) of 3.4MDa. (D) 3D reconstructed cryo-EM density maps of DCFHP, refined with octahedral symmetry. (E) Similar robust neutralization of Wuhan-1 SARS-CoV-2 pseudovirus with day 21 serum from mice immunized with either SΔC-Fer or DCFHP formulated with 500 μg alum and 20 μg CpG 1826, following a single immunization. Neutralization titers were assessed in a HeLa cell line expressing ACE2 and TMPRSS2. Data for 10 mice are presented as geometric mean titer and standard deviation. Assay limit of quantitation (LOQ) is shown as a dotted horizontal line.

Finally, mice immunized with either SΔC-Fer or DCFHP, adjuvanted with a high dose of alum and CpG, showed highly robust and similar immunogenic profiles by enzyme-linked immunosorbent assay (ELISA) ([SI Fig 2A](#)) and pseudoviral neutralization assays⁴⁴ ([Fig 1E](#)); see also³⁰.

DCFHP formulated with alum is highly immunogenic and stable at elevated temperatures

Given the robust immunogenicity of DCFHP formulated with alum and CpG, we hypothesized that the use of alum as the sole adjuvant for DCFHP (i.e., DCFHP-alum) might still elicit a robust response. Indeed, though the response was diminished compared to alum + CpG, DCFHP-alum elicited

strong pseudoviral neutralizing titers of approximately 10^4 in mice ([SI Fig 2B](#)). Under these conditions, DCFHP is 100% bound to alum³⁰.

To investigate the stability of the DCFHP-alum vaccine, samples were stored at 4°C, 27°C, or 37°C for varying times and the immunogenicity of these stored samples was evaluated in a single-dose mouse immunization study. Remarkably, the DCFHP-alum vaccine remained similarly immunogenic across all temperatures and storage periods, as measured in pseudoviral neutralization assays ([Fig 2](#)). We conclude that DCFHP-alum is stable, as measured by mice immunogenicity studies, after storage for at least two weeks at 37°C.

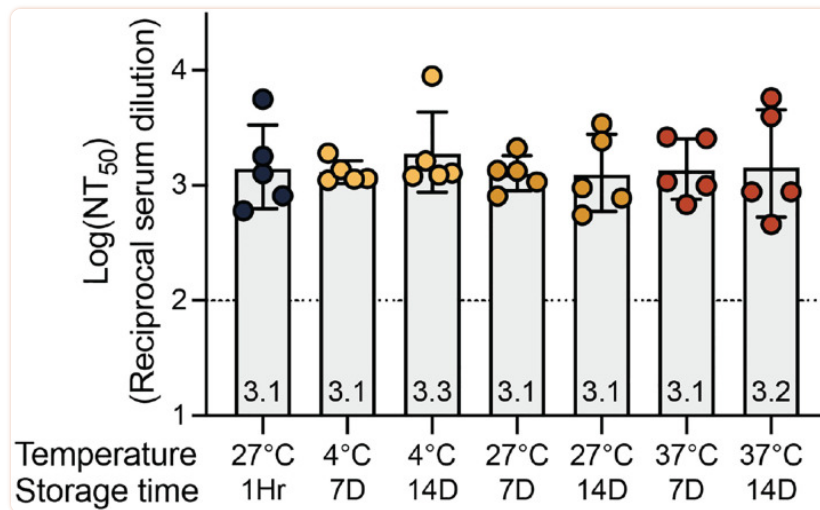


[Figure 2 –](#)

Formulated DCFHP-alum is thermostable up to 37 °C for 14 days. Neutralization titers against Wuhan-1 SARS-CoV-2 pseudovirus for serum obtained from individual animals 21 days following immunization with DCFHP-alum (10 µg DCFHP with 150 µg alum) that had been stored at a range of temperatures (bottom) for either 7 days or 14 days, compared to freshly formulated DCFHP-alum (left, black circles). Assay limits of quantitation is shown as a dotted horizontal line.

Stable expression of DCFHP increases yield and simplifies purification

To facilitate future manufacturing of DCFHP under good manufacturing practices (GMP) conditions, we next aimed to develop a high-producing stable mammalian cell line expressing DCFHP. To do so, multiple copies of a codon-optimized DCFHP gene were inserted into CHO-K1 cells using a Leap-In transposase at ATUM,^{45,46} a bioengineering company (see [Methods](#)). As anticipated⁴⁷, N-glycosylation profiles of these proteins expressed transiently in Expi293 versus stably in CHO cells differ³⁰ but they are similarly immunogenic in mice, as measured in pseudoviral neutralization assays³⁰. Following preliminary analysis of expression in pooled cells, 125 single-cell clones were evaluated for high levels of cell growth and productivity, resulting in 24 lead clones ([SI Fig 3A–C](#)). Among these, we chose clones ([SI Fig 4A–C](#)) that showed favorable expression and nanoparticle assembly, as determined by SDS-PAGE, biolayer interferometry (BLI), and SEC-MALS ([SI Fig 3A–C](#), respec-

tively). In this manner, we identified five CHO-K1 stable cell clones ([SI Fig 4A](#)) that express DCFHP at a high nanoparticle:monomer ratio ([SI Fig 4B](#)), with expected stability ([SI Fig 4C](#)), and exceptional yield (>2 g/L, [Fig 4A](#)).

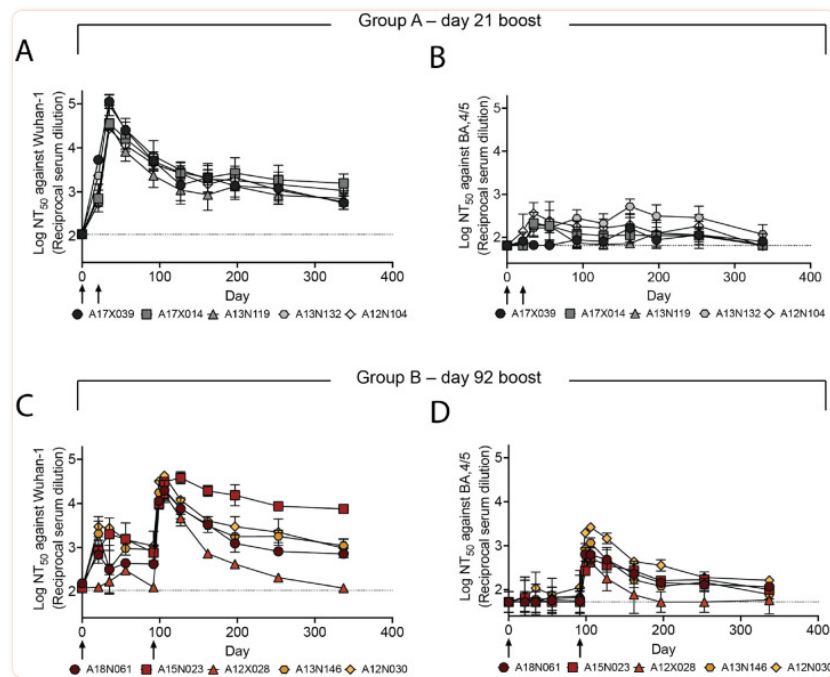


Figure 4 –

DCFHP-alum immunized NHPs elicit long-lived immunity against both Wuhan-1 and BA.4/5 pseudoviruses. (A) Serum neutralizing titers were monitored over 337 days against Wuhan-1 SARS-CoV-2 pseudovirus for animals in group A; days of prime and boost indicated with arrows. (B) As in panel A but against BA.4/5 pseudovirus. (C) and (D) as in panels A and B but with group B NHPs, respectively. Averages and standard deviations for replicate neutralization assays are shown; for panels A-D: n = 3, n = 4, n = 2 and n = 3, respectively. NHP identification provided correlate with [SI table 1](#). Assay limits of quantitation indicated by horizontal dotted lines.

Additionally, we were able to optimize the purification of the nanoparticles over our previous method¹⁴. The CHO cell-derived supernatant was supplemented to 200mM sodium chloride and flowed over a HiTrapQ anion-exchange column. The nanoparticle-containing flowthrough was concentrated and subjected to size exclusion chromatography purification (see [Methods](#)). These changes enabled rapid and simplified nanoparticle purification, with increased yield, while maintaining high overall purity.

DCFHP-alum is robustly immunogenic in non-human primates (NHPs)

Encouraged by results demonstrating that sera from mice immunized with DCFHP-alum showed potent neutralizing activity against SARS-CoV-2 pseudovirus, we sought to investigate the immunogenicity of the DCFHP-alum vaccine in NHPs. DCFHP purified from engineered CHO-K1 cells was used for the immunization of ten male rhesus macaques, aged between 3 and 9 years ([SI Table 1](#)).

The ten NHPs were divided into two groups to test the effect of a short and a long gap between the primary and booster doses. Longer gaps have been found to produce more robust immune responses in other vaccines.⁴⁸

We primed both NHP groups on day 0 and boosted at either day 21 (group A) or day 92 (group B) ([Fig 3A](#) and [SI Table 2](#)). DCFHP-alum elicited a neutralizing immune response 21 days after a single immunization in both groups ([Fig 3B](#)). While the response was substantially improved following a booster dose in both groups, the delayed boost elicited better neutralizing antisera, as assessed 14 days post boost ([Fig 3C](#) and [D](#); [SI Table 3](#)); on average, group B showed approximately a 4-fold increased neutralizing response relative to group A against divergent VOCs. Remarkably, DCFHP-alum vaccination of NHPs also elicits robust neutralization of pseudotyped SARS-CoV-1 ([Fig 3C](#) and [D](#)), which is distant from SARS-CoV-2 on the betasarbecovirus phylogenetic tree.³⁹

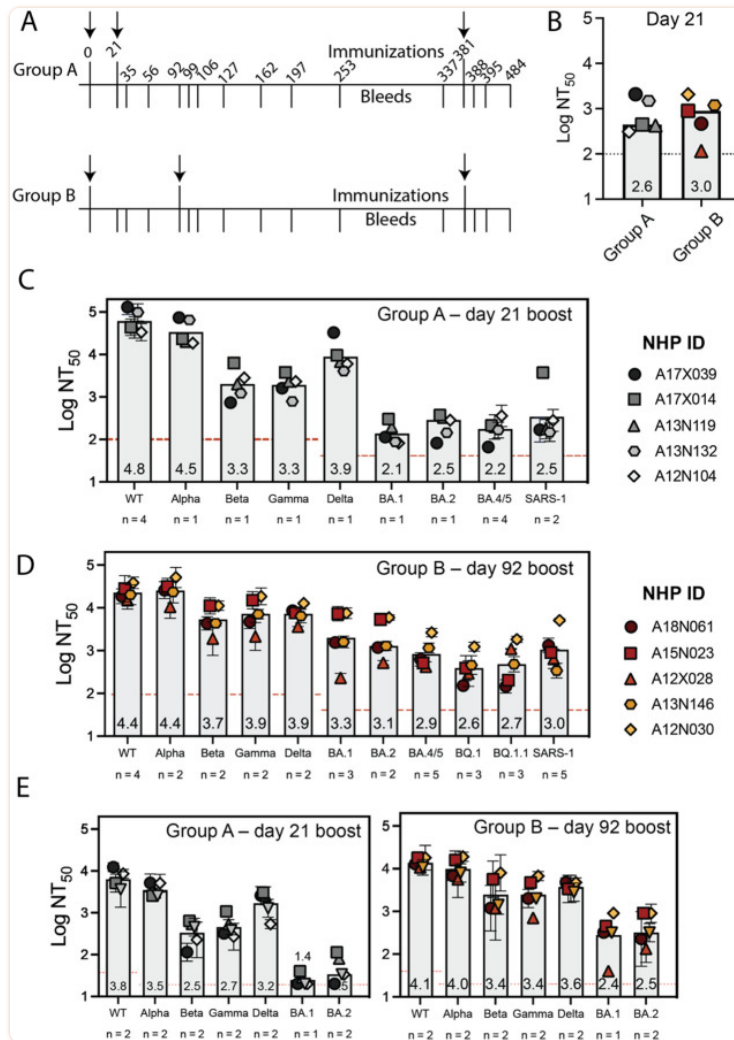


Figure 3 –

DCFHP-alum immunized NHPs elicit cross-reactive neutralizing responses. (A) Immunization scheme for NHPs immunized in either group A or group B with a 50 µg dose of DCFHP formulated with 750 µg alum (SI Table 2). Arrows indicate days of immunization. (B) Pseudoviral neutralization (plotted as the log of the neutralizing titer (reciprocal serum dilution)) of Wuhan-1 SARS-CoV-2 from NHP serum obtained 21 days following initial immunization are similar between groups A and B. (C) Cross-reactive pseudoviral neutralization by serum from NHPs isolated 14 days post boost. Means and standard deviations for biological replicates are plotted and noted for each animal (n = number of biological replicates). (D) As in panel C for group B. (E) Limited dilution, neutralization values for authentic SARS-CoV-2 VOCs for serum samples obtained 14 days post-boost. NHP identification provided correlate with SI Table 1. Assay limits of quantitation indicated by horizontal dotted line.

When tested against authentic SARS-CoV-2 virus, consistent with the results in pseudoviral assays, sera from the NHPs showed neutralization against the Wuhan-1 virus and VOCs (Fig 3E). Notably, a ferritin-based SARS-CoV-2 vaccine candidate that elicits similar neutralizing titers to those described here has been shown to confer protection in hamster⁴⁹ and NHP challenge models.¹⁶

Long-lived immune responses in non-human primates

We further investigated the durability of the vaccine-induced neutralizing responses elicited in groups A and B ([Fig 4A–D](#), [SI Fig 5](#), [SI Table 2](#)). Notably, all NHPs maintained a neutralizing anti-serum response against the Wuhan-1 pseudovirus persisting for at least 250 days ([Fig 4A](#) and [C](#)). Similarly, albeit more modestly, most animals in group B retained detectable neutralizing potency against BA.4/5 and the sequence-divergent SARS-CoV-1 out to one year ([Fig 4D](#) and [SI Fig 5B](#)), with titers generally higher than seen in group A ([Fig 4B](#) and [D](#) and [SI Fig 5A](#) and [B](#)).

Simple modeling suggests a biphasic decay of neutralizing activity against Wuhan-1 pseudovirus following the boost for group A (days 35 – 337) with an initial, fast-phase (half-life of ~5 weeks) followed by a slow-phase (half-life of several years) ([Fig 4](#), [SI Fig 6B](#) and [SI Table 4](#)). The fast-phase accounts for approximately 50% of the total decay ([SI Fig 6B](#) and [SI Table 4](#)). Simple modeling of these data with a single-phase decay shows a half-life of one year, with a poorer fit than for biphasic decay ([SI Fig 6A](#) and [SI Table 4](#)). Similar trends are seen following the boost for group B (days 106 – 337), although with greater variability, presumably because our long-term data for group B is sparse ([SI Table 4](#)). In either case, a substantial portion of the serum neutralizing activity appears to decay very slowly with time following immunization of NHPs with DCFHP-alum.

To explicitly test the potential of DCFHP-alum as an annual vaccine, we gave a second boost to all NHPs on day 381. Animals in both groups A and B showed a strong anamnestic immune response with average NT_{50} values against Wuhan-1, BA.4/5, SARS-CoV-1, and BQ.1 of approximately 10^4 , $10^{3.5}$, 10^3 , and 10^3 respectively ([Fig 5A–H](#), data for BQ.1.1 shown in [SI Fig 7](#)). The responses for the animals in group A is particularly striking given that their responses had generally waned prior to the second boost (compare [Fig. 4A](#) and [B](#) and [SI Fig 5A](#) to [Fig. 5 A–C](#)).

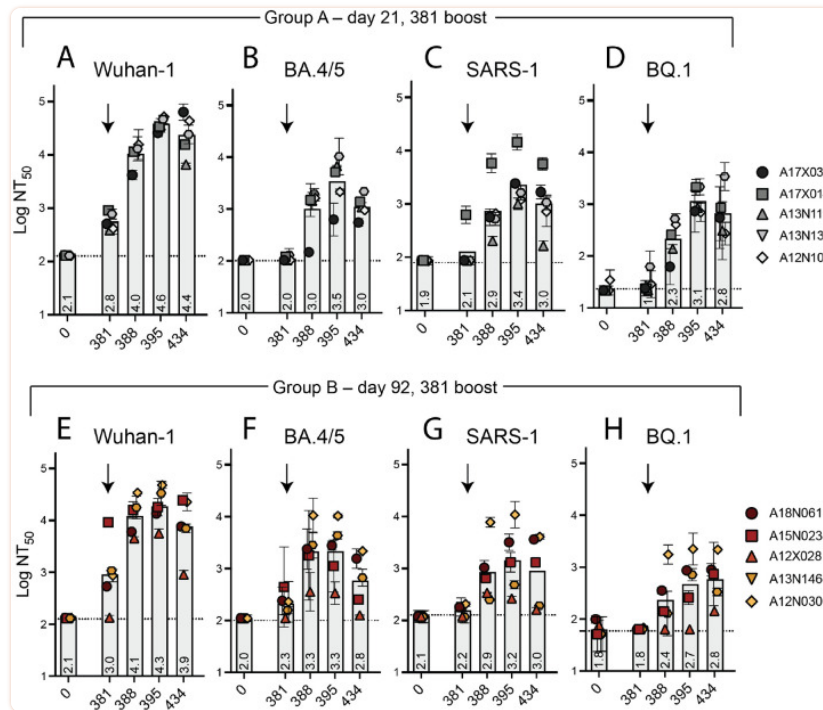


[Figure 5 –](#)

Robust serum neutralizing anamnestic responses following a second booster of DCFHP-alum after one year in NHPs. (A) Pseudovirus neutralization against Wuhan-1 (A), BA.4/5 (B), SARS-1 (C), or BQ.1 (D) by antisera from NHPs in group A following a boost at day 381. Days shown on x axis. (E)-(H) as in panels A-D but with NHPs in group B. NHP identification provided correlate with [SI table 1](#). (n = 2 biological replicates throughout). Assay limits of quantitation indicated by horizontal dotted lines.

As seen previously for with immune responses with protein-based vaccines in a naive population,⁵⁰ we observed a dominant CD4⁺ T cell response with no detectable CD8⁺ T cell response. In both groups, DCFHP-alum elicited a balanced distribution of Th1 and Th2 CD4⁺ T cells ([Fig 6A–D](#), and [SI Fig. 8](#)). This response was similar to those reported for previous COVID-19 nanoparticle vaccines and with other adjuvant formulations.⁵⁰ Importantly, we detected responses from peptides derived not only from the original Wuhan-1 strain ([Fig 6A](#) and [C](#)), but also from the Omicron BA.1 strain ([Fig 6B](#) and [D](#)), suggesting responses targeting conserved T cell epitopes.

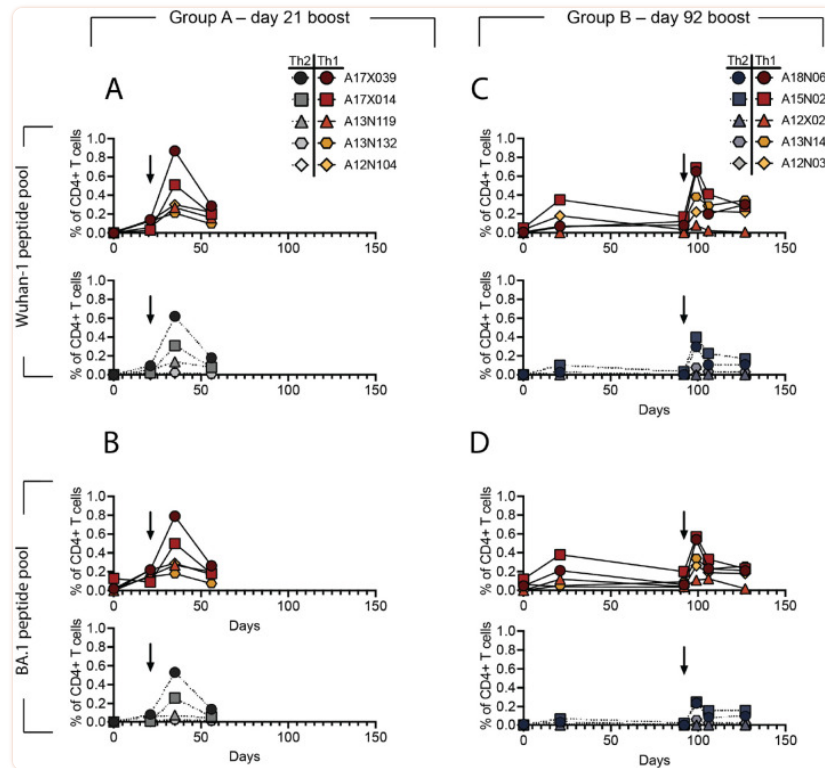


Figure 6 –

DCFHP-alum immunized NHPs shows a balanced distribution of Th1 and Th2 CD4+ T cell responses. T cells from animals in group A, isolated on the day shown on the x-axis, were stimulated with a peptide pool derived from Wuhan-1 (A) or Omicron BA.1 (B) spike protein and Th1 (top) and Th2 (bottom) cytokines were measured using flow cytometry (SI Fig. 8). Percent of CD4+ T cells that express either Th1 (IL-2,IFN γ or TNF α) (yellows and reds) or Th2 (IL-4) (greys) cytokines following stimulation shows both are elicited following vaccination with DCFHP-alum. Arrow denotes day of boost. (C)-(D) As in panels A-B but with NHPs in group B. NHP identification provided correlate with SI table 1.

DISCUSSION:

Our DCFHP-alum vaccine candidate, despite being based solely on the ancestral Wuhan-1 sequence, can elicit a robust, broad-spectrum neutralizing antiserum response in NHPs against SARS-CoV-2 VOCs, as well as against SARS-CoV-1, that is durable for >250 days. These findings challenge the notion that bivalent vaccines are required to address the COVID-19 pandemic. In addition, while there is continued discussion surrounding annual COVID-19 vaccine boosters,⁵¹⁻⁵³ little to no work has been done to test the capacity of vaccines to elicit neutralizing antibody responses with durability of one year and to elicit a subsequent response following an annual booster dose. Our results show that DCFHP-alum can elicit durable, broad-spectrum neutralizing antisera (including against BA.4/5, BQ.1, and SARS-CoV-1) in NHPs. We also show that a robust, anamnestic response can be elicited following a second boost after one year.

Several studies of COVID-19 vaccines have established that a cell-culture pseudovirus neutralizing titer of $\sim 10^2$ translates into human vaccine efficacy against symptomatic disease of $\sim 90\%$.^{52–56} In addition, clinical trials have established a correlation between anti-SARS-CoV-2 monoclonal antibody levels (i.e., humoral immunity alone) and protection from COVID-19.^{57,58} Indeed, SARS-CoV-2 variant booster vaccines have been accepted by the FDA and EMA for emergency use authorization using neutralizing antibody titer as a correlate of protection.^{59,60}

Accordingly, if our NHP results are reproduced in clinical trials, we anticipate that DCFHP-alum could be widely used as a booster vaccine for individuals who have been previously vaccinated with other COVID-19 vaccines, and in unvaccinated individuals that have been previously infected with SARS-CoV-2. Together, these two categories encompass a large fraction of the world's population. As such, DCFHP-alum would be an attractive annual vaccine that could circumvent the need for continual variant chasing.

We also envision that DCFHP-alum could enable global access to COVID-19 vaccination given its low projected cost of goods, high scale of production, and favorable broad-spectrum profile. Our results show that a DCFHP stably integrated CHO-based cell line could enable low-cost, large-scale production. Assuming a vaccine dose of ≤ 100 micrograms and a purification yield of $\geq 10\%$, we anticipate production of thousands of DCFHP vaccine doses per liter of engineered CHO-K1 cell culture. As well, the DCFHP-alum formulation is stable for at least two weeks at temperatures exceeding standard room temperature. Taken together, DCFHP-alum is an excellent candidate for development as a new COVID-19 vaccine, offering broad-spectrum protection, and providing the opportunity for global access without the cold chain distribution challenges encountered with other vaccines.⁶¹

Finally, we anticipate the potential use of DCFHP-alum as an important primary vaccine in previously unvaccinated and uninfected individuals, especially in pediatric populations, including infants. Aluminum salt adjuvants are commonly used in infant vaccines and as part of routine childhood immunization schedules, and their excellent safety profile has been established over decades.^{31–36} In infants and other DCFHP-alum vaccine recipients naïve to SARS-CoV-2 infection or vaccination, we would anticipate robust, cross-reactive responses similar to the naïve NHPs studied here. Since primary immunization of NHPs with DCFHP-alum provides remarkably broad protection against VOCs, DCFHP-alum may be an ideal way to establish initial immune imprinting^{62–64} against SARS-CoV-2 in infants.

Supplementary Material

ACKNOWLEDGMENTS:

We thank members of the Kim Lab for discussions, and Dr. Luciana Borio and Dr. Duo Xu for helpful comments on an earlier draft of this manuscript. S.T. acknowledges NIH NICHD grant K99HD104924 and the Merck fellowship from the Damon Runyon Cancer Research Foundation. The CryoEM microscopy work was performed at the Stanford-SLAC Cryo-EM Center (S2C2) supported by the NIH Common Fund Transformative High Resolution Cryo-Electron Microscopy program (U24 GM129541). We thank F. Krammer and F. Amanat for providing the SARS-CoV-2 RBD plasmids for protein production, and J. Bloom and A. Greaney for plasmids and cells related to viral neutralization assays. The findings and conclusions in this article are those of the author(s) and do not necessarily represent the views or opinions of the California Department of Public Health or the California Health and Human Services Agency. This work was supported by the Frank Quattrone & Denise Foderaro Family Research Fund, the Chan Zuckerberg Biohub, the Stanford Innovative Medicines Accelerator, the Virginia & D.K. Ludwig Fund for Cancer Research, and an NIH Director's Pioneer Award (DP1AI158125) to P.S.K.

Footnotes

COMPETING INTERESTS:

P.A.B.W., M.S., N.F., S.T. and P.S.K. are named as inventors on patent applications applied for by Stanford University and the Chan Zuckerberg Biohub on immunogenic coronavirus fusion proteins and related methods, which have been licensed to Vaccine Company, Inc. P.A.B.W. is an employee of, and P.S.K. is a co-founder of Vaccine Company, Inc.

REFERENCES:

1. Polack F. P. et al. Safety and Efficacy of the BNT162b2 mRNA Covid-19 Vaccine. *N Engl J Med* 383, 2603–2615 (2020). 10.1056/NEJMoa2034577 [[PMC free article](#)] [[PubMed](#)] [[CrossRef](#)] [[Google Scholar](#)]
2. Walsh E. E. et al. Safety and Immunogenicity of Two RNA-Based Covid-19 Vaccine Candidates. *N Engl J Med* 383, 2439–2450 (2020). 10.1056/NEJMoa2027906 [[PMC free article](#)] [[PubMed](#)] [[CrossRef](#)] [[Google Scholar](#)]
3. Watson O. J. et al. Global impact of the first year of COVID-19 vaccination: a mathematical modelling study. *Lancet Infect Dis* 22, 1293–1302 (2022). 10.1016/S1473-3099(22)00320-6 [[PMC free article](#)] [[PubMed](#)] [[CrossRef](#)] [[Google Scholar](#)]
4. Shrotri M., Swinnen T., Kampmann B. & Parker E. P. K. An interactive website tracking COVID-19 vaccine development. *Lancet Glob Health* 9, e590–e592 (2021). 10.1016/S2214-109X(21)00043-7 [[PMC free article](#)] [[PubMed](#)] [[CrossRef](#)] [[Google Scholar](#)]
5. Acharya K. P., Ghimire T. R. & Subramanya S. H. Access to and equitable distribution of COVID-19 vaccine in low-income countries. *NPJ Vaccines* 6, 54 (2021). 10.1038/s41541-021-00323-6 [[PMC free article](#)] [[PubMed](#)] [[CrossRef](#)] [[Google Scholar](#)]
6. Kumru O. S. et al. Vaccine instability in the cold chain: mechanisms, analysis and formulation strategies. *Biologicals* 42, 237–259 (2014). 10.1016/j.biologicals.2014.05.007 [[PubMed](#)] [[CrossRef](#)] [[Google Scholar](#)]

7. Levin E. G. et al. Waning Immune Humoral Response to BNT162b2 Covid-19 Vaccine over 6 Months. *N Engl J Med* 385, e84 (2021). 10.1056/NEJMoa2114583 [[PMC free article](#)] [[PubMed](#)] [[CrossRef](#)] [[Google Scholar](#)]
8. Cele S. et al. Omicron extensively but incompletely escapes Pfizer BNT162b2 neutralization. *Nature* 602, 654–656 (2022). 10.1038/s41586-021-04387-1 [[PMC free article](#)] [[PubMed](#)] [[CrossRef](#)] [[Google Scholar](#)]
9. Kaslow D. C. et al. Why vaccinate children against COVID-19? *Vaccine Insights* 1, 213–218 (2022). 10.18609/vac.2022.32 [[CrossRef](#)] [[Google Scholar](#)]
10. Zhao L. et al. Nanoparticle vaccines. *Vaccine* 32, 327–337 (2014). 10.1016/j.vaccine.2013.11.069 [[PubMed](#)] [[CrossRef](#)] [[Google Scholar](#)]
11. Lopez-Sagaseta J., Malito E., Rappuoli R. & Bottomley M. J. Self-assembling protein nanoparticles in the design of vaccines. *Comput Struct Biotechnol J* 14, 58–68 (2016). 10.1016/j.csbj.2015.11.001 [[PMC free article](#)] [[PubMed](#)] [[CrossRef](#)] [[Google Scholar](#)]
12. Kelly H. G., Kent S. J. & Wheatley A. K. Immunological basis for enhanced immunity of nanoparticle vaccines. *Expert Rev Vaccines* 18, 269–280 (2019). 10.1080/14760584.2019.1578216 [[PubMed](#)] [[CrossRef](#)] [[Google Scholar](#)]
13. Cohen A. A. et al. Mosaic nanoparticles elicit cross-reactive immune responses to zoonotic coronaviruses in mice. *Science* 371, 735–741 (2021). 10.1126/science.abf6840 [[PMC free article](#)] [[PubMed](#)] [[CrossRef](#)] [[Google Scholar](#)]
14. Powell A. E. et al. A Single Immunization with Spike-Functionalized Ferritin Vaccines Elicits Neutralizing Antibody Responses against SARS-CoV-2 in Mice. *ACS Cent Sci* 7, 183–199 (2021). 10.1021/acscentsci.0c01405 [[PMC free article](#)] [[PubMed](#)] [[CrossRef](#)] [[Google Scholar](#)]
15. Joyce M. G. et al. SARS-CoV-2 ferritin nanoparticle vaccines elicit broad SARS coronavirus immunogenicity. *Cell Rep* 37, 110143 (2021). 10.1016/j.celrep.2021.110143 [[PMC free article](#)] [[PubMed](#)] [[CrossRef](#)] [[Google Scholar](#)]
16. Joyce M. G. et al. A SARS-CoV-2 ferritin nanoparticle vaccine elicits protective immune responses in nonhuman primates. *Sci Transl Med* 14, eabi5735 (2022). 10.1126/scitranslmed.abi5735 [[PubMed](#)] [[CrossRef](#)] [[Google Scholar](#)]
17. Swanson K. A. et al. A respiratory syncytial virus (RSV) F protein nanoparticle vaccine focuses antibody responses to a conserved neutralization domain. *Sci Immunol* 5 (2020). 10.1126/sciimmunol.aba6466 [[PubMed](#)] [[CrossRef](#)] [[Google Scholar](#)]
18. Sliepen K. et al. Presenting native-like HIV-1 envelope trimers on ferritin nanoparticles improves their immunogenicity. *Retrovirology* 12, 82 (2015). 10.1186/s12977-015-0210-4 [[PMC free article](#)] [[PubMed](#)] [[CrossRef](#)] [[Google Scholar](#)]
19. Yassine H. M. et al. Hemagglutinin-stem nanoparticles generate heterosubtypic influenza protection. *Nat Med* 21, 1065–1070 (2015). 10.1038/nm.3927 [[PubMed](#)] [[CrossRef](#)] [[Google Scholar](#)]
20. Kanekiyo M. et al. Rational Design of an Epstein-Barr Virus Vaccine Targeting the Receptor-Binding Site. *Cell* 162, 1090–1100 (2015). 10.1016/j.cell.2015.07.043 [[PMC free article](#)] [[PubMed](#)] [[CrossRef](#)] [[Google Scholar](#)]
21. Bu W. et al. Immunization with Components of the Viral Fusion Apparatus Elicits Antibodies That Neutralize Epstein-Barr Virus in B Cells and Epithelial Cells. *Immunity* 50, 1305–1316 e1306 (2019). 10.1016/j.immuni.2019.03.010 [[PMC free article](#)] [[PubMed](#)] [[CrossRef](#)] [[Google Scholar](#)]
22. Houser K. V. et al. Safety and immunogenicity of a ferritin nanoparticle H2 influenza vaccine in healthy adults: a phase 1 trial. *Nat Med* 28, 383–391 (2022). 10.1038/s41591-021-01660-8 [[PMC free article](#)] [[PubMed](#)] [[CrossRef](#)] [[Google Scholar](#)]

23. Pallesen J. et al. Immunogenicity and structures of a rationally designed prefusion MERS-CoV spike antigen. *Proc Natl Acad Sci U S A* 114, E7348–E7357 (2017). 10.1073/pnas.1707304114 [[PMC free article](#)] [[PubMed](#)] [[CrossRef](#)] [[Google Scholar](#)]
24. Jackson L. A. et al. An mRNA Vaccine against SARS-CoV-2 - Preliminary Report. *N Engl J Med* 383, 1920–1931 (2020). 10.1056/NEJMoa2022483 [[PMC free article](#)] [[PubMed](#)] [[CrossRef](#)] [[Google Scholar](#)]
25. Walls A. C. et al. Structure, Function, and Antigenicity of the SARS-CoV-2 Spike Glycoprotein. *Cell* 181, 281–292 e286 (2020). 10.1016/j.cell.2020.02.058 [[PMC free article](#)] [[PubMed](#)] [[CrossRef](#)] [[Google Scholar](#)]
26. Hsieh C. L. et al. Structure-based design of prefusion-stabilized SARS-CoV-2 spikes. *Science* 369, 1501–1505 (2020). 10.1126/science.abd0826 [[PMC free article](#)] [[PubMed](#)] [[CrossRef](#)] [[Google Scholar](#)]
27. Wrapp D. et al. Cryo-EM structure of the 2019-nCoV spike in the prefusion conformation. *Science* 367, 1260–1263 (2020). 10.1126/science.abb2507 [[PMC free article](#)] [[PubMed](#)] [[CrossRef](#)] [[Google Scholar](#)]
28. Zamecnik C. R. et al. ReScan, a Multiplex Diagnostic Pipeline, Pans Human Sera for SARS-CoV-2 Antigens. *Cell Rep Med* 1, 100123 (2020). 10.1016/j.xcrm.2020.100123 [[PMC free article](#)] [[PubMed](#)] [[CrossRef](#)] [[Google Scholar](#)]
29. Li Y. et al. Linear epitope landscape of the SARS-CoV-2 Spike protein constructed from 1,051 COVID-19 patients. *Cell Rep* 34, 108915 (2021). 10.1016/j.celrep.2021.108915 [[PMC free article](#)] [[PubMed](#)] [[CrossRef](#)] [[Google Scholar](#)]
30. Kumru O. S., Friedland N., Sanyal M., Hickey J., Joshi R., Weidenbacher P., Kim P. S., Joshi S. B., Volkin D. B. . Formulation development and comparability studies with an aluminum-salt adjuvanted SARS-CoV-2 Spike ferritin nanoparticle vaccine antigen produced from two different cell lines. *In Preparation* (2022). [[PMC free article](#)] [[PubMed](#)] [[Google Scholar](#)]
31. De Gregorio E., Tritto E. & Rappuoli R. Alum adjuvanticity: unraveling a century old mystery. *Eur J Immunol* 38, 2068–2071 (2008). 10.1002/eji.200838648 [[PubMed](#)] [[CrossRef](#)] [[Google Scholar](#)]
32. Di Pasquale A., Preiss S., Tavares Da Silva F. & Garçon N. Vaccine Adjuvants: from 1920 to 2015 and Beyond. *Vaccines (Basel)* 3, 320–343 (2015). 10.3390/vaccines3020320 [[PMC free article](#)] [[PubMed](#)] [[CrossRef](#)] [[Google Scholar](#)]
33. HogenEsch H., O'Hagan D. T. & Fox C. B. Optimizing the utilization of aluminum adjuvants in vaccines: you might just get what you want. *NPJ Vaccines* 3, 51 (2018). 10.1038/s41541-018-0089-x [[PMC free article](#)] [[PubMed](#)] [[CrossRef](#)] [[Google Scholar](#)]
34. Tritto E., Mosca F. & De Gregorio E. Mechanism of action of licensed vaccine adjuvants. *Vaccine* 27, 3331–3334 (2009). 10.1016/j.vaccine.2009.01.084 [[PubMed](#)] [[CrossRef](#)] [[Google Scholar](#)]
35. Mitkus R. J., King D. B., Hess M. A., Forshee R. A. & Walderhaug M. O. Updated aluminum pharmacokinetics following infant exposures through diet and vaccination. *Vaccine* 29, 9538–9543 (2011). 10.1016/j.vaccine.2011.09.124 [[PubMed](#)] [[CrossRef](#)] [[Google Scholar](#)]
36. Baylor N. W., Egan W. & Richman P. Aluminum salts in vaccines--US perspective. *Vaccine* 20 Suppl 3, S18–23 (2002). 10.1016/s0264-410x(02)00166-4 [[PubMed](#)] [[CrossRef](#)] [[Google Scholar](#)]
37. Tuekprakhon A. et al. Antibody escape of SARS-CoV-2 Omicron BA.4 and BA.5 from vaccine and BA.1 serum. *Cell* 185, 2422–2433 e2413 (2022). 10.1016/j.cell.2022.06.005 [[PMC free article](#)] [[PubMed](#)] [[CrossRef](#)] [[Google Scholar](#)]
38. Qu P. et al. Distinct Neutralizing Antibody Escape of SARS-CoV-2 Omicron Subvariants BQ.1, BQ.1.1, BA.4.6, BF.7 and BA.2.75.2. *bioRxiv*, 2022.2010.2019.512891 (2022). 10.1101/2022.10.19.512891 [[CrossRef](#)] [[Google Scholar](#)]

39. Jaimes J. A., Andre N. M., Chappie J. S., Millet J. K. & Whittaker G. R. Phylogenetic Analysis and Structural Modeling of SARS-CoV-2 Spike Protein Reveals an Evolutionary Distinct and Proteolytically Sensitive Activation Loop. *J Mol Biol* 432, 3309–3325 (2020). 10.1016/j.jmb.2020.04.009 [[PMC free article](#)] [[PubMed](#)] [[CrossRef](#)] [[Google Scholar](#)]
40. Tian X. et al. Potent binding of 2019 novel coronavirus spike protein by a SARS coronavirus-specific human monoclonal antibody. *Emerg Microbes Infect* 9, 382–385 (2020). 10.1080/22221751.2020.1729069 [[PMC free article](#)] [[PubMed](#)] [[CrossRef](#)] [[Google Scholar](#)]
41. Brouwer P. J. M. et al. Potent neutralizing antibodies from COVID-19 patients define multiple targets of vulnerability. *Science* 369, 643–650 (2020). 10.1126/science.abc5902 [[PMC free article](#)] [[PubMed](#)] [[CrossRef](#)] [[Google Scholar](#)]
42. Sauer M. M. et al. Structural basis for broad coronavirus neutralization. *Nat Struct Mol Biol* 28, 478–486 (2021). 10.1038/s41594-021-00596-4 [[PubMed](#)] [[CrossRef](#)] [[Google Scholar](#)]
43. Shang J. et al. Cell entry mechanisms of SARS-CoV-2. *Proc Natl Acad Sci U S A* 117, 11727–11734 (2020). 10.1073/pnas.2003138117 [[PMC free article](#)] [[PubMed](#)] [[CrossRef](#)] [[Google Scholar](#)]
44. Crawford K. H. D. et al. Protocol and Reagents for Pseudotyping Lentiviral Particles with SARS-CoV-2 Spike Protein for Neutralization Assays. *Viruses* 12 (2020). 10.3390/v12050513 [[PMC free article](#)] [[PubMed](#)] [[CrossRef](#)] [[Google Scholar](#)]
45. Balasubramanian S. et al. Generation of High Expressing Chinese Hamster Ovary Cell Pools Using the Leap-In Transposon System. *Biotechnol J* 13, e1700748 (2018). 10.1002/biot.201700748 [[PubMed](#)] [[CrossRef](#)] [[Google Scholar](#)]
46. Rajendran S. et al. Accelerating and de-risking CMC development with transposon-derived manufacturing cell lines. *Biotechnol Bioeng* 118, 2301–2311 (2021). 10.1002/bit.27742 [[PMC free article](#)] [[PubMed](#)] [[CrossRef](#)] [[Google Scholar](#)]
47. Croset A. et al. Differences in the glycosylation of recombinant proteins expressed in HEK and CHO cells. *J Biotechnol* 161, 336–348 (2012). 10.1016/j.jbiotec.2012.06.038 [[PubMed](#)] [[CrossRef](#)] [[Google Scholar](#)]
48. Ledgerwood J. E. et al. Prime-boost interval matters: a randomized phase 1 study to identify the minimum interval necessary to observe the H5 DNA influenza vaccine priming effect. *J Infect Dis* 208, 418–422 (2013). 10.1093/infdis/jit180 [[PMC free article](#)] [[PubMed](#)] [[CrossRef](#)] [[Google Scholar](#)]
49. Wuertz K. M. et al. A SARS-CoV-2 spike ferritin nanoparticle vaccine protects hamsters against Alpha and Beta virus variant challenge. *NPJ Vaccines* 6, 129 (2021). 10.1038/s41541-021-00392-7 [[PMC free article](#)] [[PubMed](#)] [[CrossRef](#)] [[Google Scholar](#)]
50. Arunachalam P. S. et al. Adjuvanting a subunit COVID-19 vaccine to induce protective immunity. *Nature* 594, 253–258 (2021). 10.1038/s41586-021-03530-2 [[PubMed](#)] [[CrossRef](#)] [[Google Scholar](#)]
51. Cohen J. I. & Burbelo P. D. Reinfection With SARS-CoV-2: Implications for Vaccines. *Clin Infect Dis* 73, e4223–e4228 (2021). 10.1093/cid/ciaa1866 [[PMC free article](#)] [[PubMed](#)] [[CrossRef](#)] [[Google Scholar](#)]
52. Khoury D. S. et al. Neutralizing antibody levels are highly predictive of immune protection from symptomatic SARS-CoV-2 infection. *Nat Med* 27, 1205–1211 (2021). 10.1038/s41591-021-01377-8 [[PubMed](#)] [[CrossRef](#)] [[Google Scholar](#)]
53. Marks P. W., Gruppuso P. A. & Adashi E. Y. Urgent Need for Next-Generation COVID-19 Vaccines. *JAMA* (2022). 10.1001/jama.2022.22759 [[PubMed](#)] [[CrossRef](#)] [[Google Scholar](#)]
54. Gilbert P. B. et al. A Covid-19 Milestone Attained - A Correlate of Protection for Vaccines. *N Engl J Med* (2022). 10.1056/NEJMp2211314 [[PubMed](#)] [[CrossRef](#)] [[Google Scholar](#)]
55. McMahan K. et al. Correlates of protection against SARS-CoV-2 in rhesus macaques. *Nature* 590, 630–634 (2021). 10.1038/s41586-020-03041-6 [[PMC free article](#)] [[PubMed](#)] [[CrossRef](#)] [[Google Scholar](#)]

56. Goldblatt D., Alter G., Crotty S. & Plotkin S. A. Correlates of protection against SARS-CoV-2 infection and COVID-19 disease. *Immunol Rev* 310, 6–26 (2022). 10.1111/imr.13091 [[PMC free article](#)] [[PubMed](#)] [[CrossRef](#)] [[Google Scholar](#)]
57. Schmidt P. et al. Antibody-mediated protection against symptomatic COVID-19 can be achieved at low serum neutralizing titers. *medRxiv*, 2022.2010.2018.22281172 (2022). 10.1101/2022.10.18.22281172 [[PubMed](#)] [[CrossRef](#)] [[Google Scholar](#)]
58. Stadler E. et al. Monoclonal antibody levels and protection from COVID-19. *medRxiv*, 2022.2011.2022.22282199 (2022). 10.1101/2022.11.22.22282199 [[PMC free article](#)] [[PubMed](#)] [[CrossRef](#)] [[Google Scholar](#)]
59. U.S. Department of Health and Human Services Food and Drug Administration. *Emergency Use Authorization for Vaccines to Prevent COVID-19 Guidance for Industry* (2022).
60. European Medicines Agency Committee for Human Medicinal Products (CHMP). *Reflection paper on the regulatory requirements for vaccines intended to provide protection against variant strain(s) of SARS-CoV-2* (2022).
61. Uddin M. N. & Roni M. A. Challenges of Storage and Stability of mRNA-Based COVID-19 Vaccines. *Vaccines (Basel)* 9 (2021). 10.3390/vaccines9091033 [[PMC free article](#)] [[PubMed](#)] [[CrossRef](#)] [[Google Scholar](#)]
62. Roltgen K. et al. Immune imprinting, breadth of variant recognition, and germinal center response in human SARS-CoV-2 infection and vaccination. *Cell* 185, 1025–1040 e1014 (2022). 10.1016/j.cell.2022.01.018 [[PMC free article](#)] [[PubMed](#)] [[CrossRef](#)] [[Google Scholar](#)]
63. Rodda L. B. et al. Imprinted SARS-CoV-2-specific memory lymphocytes define hybrid immunity. *Cell* 185, 1588–1601 e1514 (2022). 10.1016/j.cell.2022.03.018 [[PMC free article](#)] [[PubMed](#)] [[CrossRef](#)] [[Google Scholar](#)]
64. Guthmiller J. J. & Wilson P. C. Harnessing immune history to combat influenza viruses. *Curr Opin Immunol* 53, 187–195 (2018). 10.1016/j.coi.2018.05.010 [[PubMed](#)] [[CrossRef](#)] [[Google Scholar](#)]